2023 IEEE International Conference on Robotics and Automation (ICRA 2023)
May 29 - June 2, 2023. London, UK

Touch Classification on Robotic Skin using Multimodal Tactile Sensing Modules

Min Jin Yang, Junhwi Cho, Hyunjo Chung, Kyungseo Park, and Jung Kim

***Abstract*— Human employs different touch patterns to convey diverse social messages; for example, a stroke is an encouragement, whereas a hit is an offense. Various tactile sensors have been developed to grant an intuitive physical interaction with a robotic system, yet many encountered limitations in achieving broad sensibility or fabricating into a large skin. This paper presents a robotic skin with multimodal tactile sensing modules to achieve broad spatiotemporal sensibility with a few sensing elements. The multimodal module is composed of a microphone and a vented screw installed on a conductive sensory domain. A multilayered fabric with a textured surface covers the sensory domain and forms a piezoresistive structure. High and low temporal components of touch elicit a micro-vibration and a conductivity change on the skin, where both are measured with multimodal modules. The measurements are each processed with short-time Fourier transform (STFT) and electrical resistance tomography (ERT) to encode two spatiotemporal feature maps, which are classified into ten touch classes using a convolutional neural network. Due to a sensibility to both high and low temporal components of touch, the skin classifies touches with an accuracy of 97.0 %, whereas only 84.7 % and 90.6 % are achieved when one type of feature map is used. Also, the skin is robust and beneficial in power consumption and fabrication since the multimodal modules are not exposed to an external stimulus and are sparsely distributed.**

I. Introduction

Touch is an intuitive non-verbal communication channel that plays an essential role in human interaction [1]. It commutes an emotion or derives a physiological response, therefore may mediate psychological intimacy, promote communication, or improve resilience to stress [2], [3]. Different touch patterns are used to communicate in different situations; for example, push to convey disgust and pat to convey sympathy [4]. Thus, the touch pattern, or touch modality, is an essential factor in interpreting a social touch and is differentiated by the spatiotemporal characteristics of the touch [5]. Human skin can sense touch and differentiate its modality with various mechanoreceptors [6]. Each mechanoreceptor is sensitive to different frequency bandwidths of touch by their different adapting rates, and spatial information is encoded by sensing the touch with multiple distributed mechanoreceptors. Thus human skin can simultaneously sense broad spatiotemporal properties of touch to distinguish the modality and interpret a social cue.

M. J. Yang, J. Cho, H. Chung, and J. Kim are with the Department of Mechanical Engineering, Korea Advanced Institute of Science and Technology, Daejeon 34141, Republic of Korea. (e-mail: lshiling@kaist.ac.kr, junhwi.cho@kaist.ac.kr, ignuschung@kaist.ac.kr, jungkim@kaist.ac.kr)

K. Park is with the Department of Mechanical Engineering, University of Illinois Urbana-Champaign, Urbana, IL 61801, USA (e-mail: kyungseo@illinois.edu)

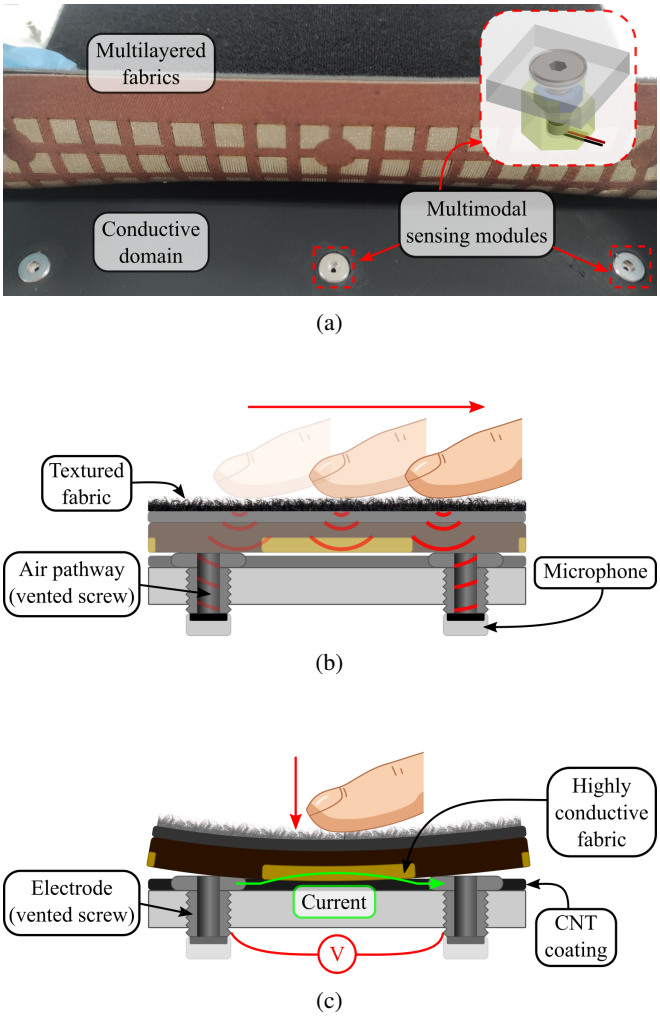

Fig. 1: Concept on the developed robotic skin. (a) The skin structure, (b-c) sensing principles of high and low temporal component of touch.

An interest in a robotic skin is continuously increasing as robotic systems rapidly advance, and start to coexist alongside a human [7]. A human can physically interact with touch and expects the robot to react intuitively like a human [8]. Therefore, a robotic skin that can differentiate various touches and understand a social message would enrich a physical human-robot interaction beyond simple somatosensory sensation to social communication in any physically interactive robotic system such as humanoids [9], [10] and social robots [11], [12].

Various tactile sensing systems have been developed to

serve as robotic skin and differentiate social touches. Requirements of robotic skin differ by application, but such systems should encode a wide range of touch's spatiotemporal properties to sense diverse touches. Also, a robotic skin should be efficiently conformed to a large scale and be robust to an external impact to stably cover the surface of a robotic system [13]. One of two common approaches in developing a large-scale conformable robotic skin that differentiates touches is forming a force-sensitive skin, such as using an array of force sensors [14] or employing a principle of electrical impedance tomography [15]. The other is making a vibration-sensitive skin using an array of piezoelectric materials [16] or measuring a structure-borne vibration with microphones [17]. Both approaches employ only one type of transducer and thus can only measure specific frequency bandwidth of touch. The prior methods have limitations in measuring high temporal stimulus, whereas the later methods cannnot measure low temporal stimulus [18], [19]. Also, the methods employing an array of transducers [14], [16] face practical limitations, such as high fabrication complexity and limited communication bandwidth, when enlarged to a large surface due to an excessive number of transducers. An alternative approach to address these limitations is modularising various transducers and a microcontroller into a tactile sensor to cover broad temporal frequencies [20]. This method classifies diverse touches and easily conforms to a large scale by connecting the modules but requires relatively large power and is fragile to external force due to exposed electronic components and wirings.

This paper presents a robotic skin using distributed multimodal tactile sensing modules to classify various social touches and to address the aforementioned limitations, such as excessive transducers and fragility. Microphones and electrodes are employed as transducers to sense touches, and an outer multilayer of a loop fabric, a neoprene foam, and a conductive fabric is fabricated to transmit touch stimuli to the transducers. Measurements from the microphones and the electrodes are each processed with discrete Fourier transform (DFT) and electrical resistance tomography (ERT) to encode spatiotemporal characteristics of touches into feature maps, and a convolutional neural network (CNN) is trained to decode and classify them. The skin senses broad frequencies and forces of thouches in a 400 cm^2 sensory domain with 25 multimodal modules and classifies a touch into ten classes with an accuracy of 97.0 %. Furthermore, the outer layer of the skin is soft, flexible, and comprises no electronic component or wiring; therefore, a large sensory domain is efficiently covered with a few sensing modules and is robust to an external impact.

II. Design and Fabrication of Multimodal Robotic Skin

Multiple transducing mechanisms are required for a tactile sensor to fully sense various touches since finding a single transducer that covers all temporal frequencies of social touches is difficult [13]. Therefore, the developed robotic skin structure is designed to employ two transducing mechanisms with different temporal sensitivity.

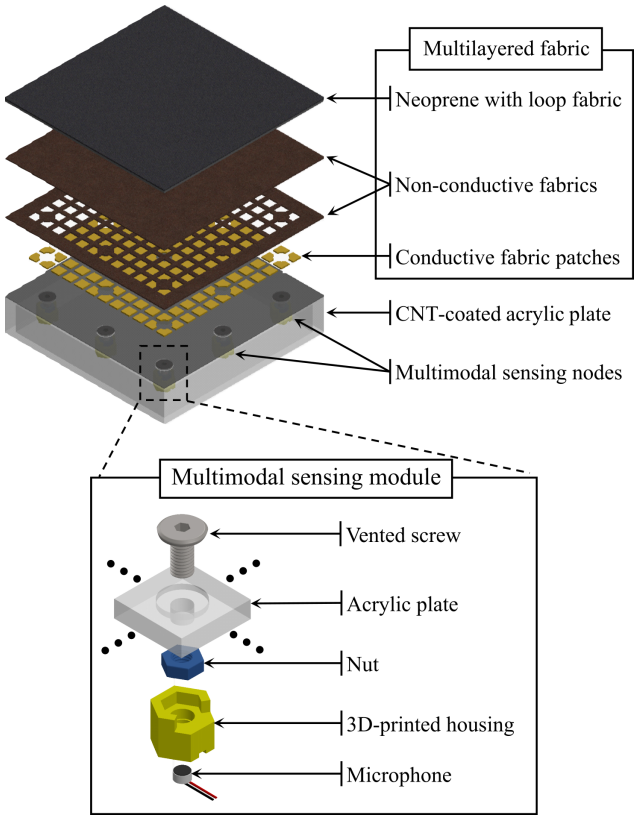

Fig. 2: Structure of the developed skin's components

A. Transducing mechanisms

A high temporal component of touch implies a dynamic component that elicits a micro-vibration on the skin, such as a moving touch across the skin or when a touch makes or breaks contact with the skin. Therefore, touches such as a stroke or pat are high temporal touch. A previous study showed that a vibratory stimulus generated on a textured skin surface could propagate and be measured by distanced transducers [17]. The proposed robotic skin is also designed with a textured surface to elicit a micro-vibration from touch and distributed microphones to sense the vibration propagated through the air.

A low temporal component of touch implies a static component that exerts sustained pressure on the skin. The pressure locally deforms a skin structure, where the deformation shape varies by the pressurised area size and strength of the pressure. A poke and press are both low temporal touches but different in pressurised area size. Previous works on ERT-based robotic skin showed a robotic skin with a piezoresistive property using conductive fabric [21]. The proposed skin is also designed with a deformable piezoresistive structure and distributed electrodes to measure conductivity in the sensory domain, which varies when the piezoresistive structure is deformed due to the low temporal pressure of touch.

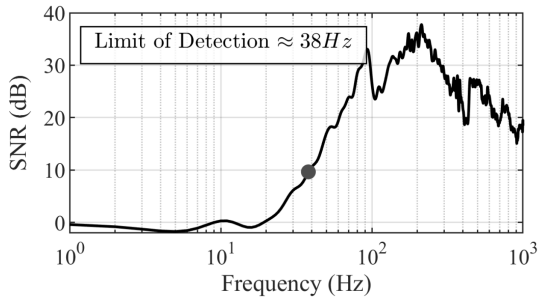

(a)

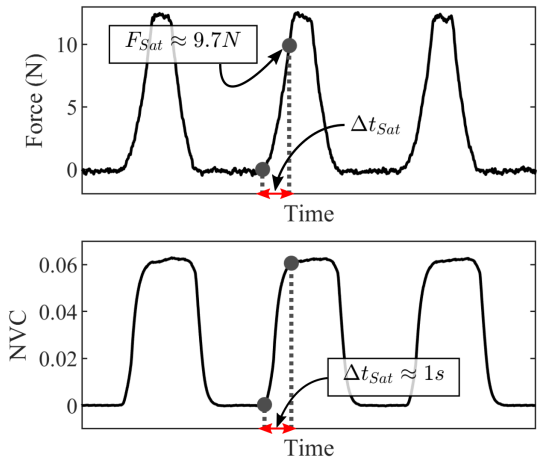

(b)

Fig. 3: The skin responses to high and low temporal stimuli. (a) Microphone signal-to-noise ratio (SNR) about vibratory stimulation frequencies and (b) applied force on the skin and the resulting normalised voltage change (NVC) in the loading-unloading test.

TABLE I: Nine touch modalities

Hit	Deliver a forcible blow with a closed fist
Pat	Gently and quickly touch with flat of hand
Poke	Jab or prod with finger
Press	Exert a steady force with flattened fingers or hand
Rub	Move hand back and forth on surface with firm pressure
Scratch	Rub with fingernails
Stroke	Move hand over with gentle pressure, often repeatedly
Tap	Strike with quick light blows using one or more fingers
Tickle	Touch with light finger movements

B. Robotic skin structure design

The developed robotic skin is composed of outer multilayered fabric and a conductive sensory domain with embedded multimodal tactile sensing modules, as shown in Fig. 2. The multilayered fabric is composed of a loop fabric, a neoprene foam, and conductive fabric patches in the outermost order. The loop fabric in the outermost layer has a textured surface, which elicits a vibration from a high temporal touch component. The neoprene foam in the middle has a resilient mechanical property and thus deforms by a low temporal touch component. The conductive fabric patches in the bottom layer are adjacent to the conductive sensory domain, making a conductivity change when pressed against the conductive sensory domain. A larger deformation by a greater pressure or a larger contact area varies the conductivity more; thus, the robotic skin acquires a piezoresistive property.

The multimodal tactile sensing module is a microphone-attached vented screw fastened on the conductive sensory domain. The microphone measures an air vibration induced on the multilayered fabric, which propagates to the microphone through an air pathway secured by the vented screw. The screw also serves as an electrode to measure a conductivity change in the sensory domain. Therefore, the screws and the conductive sensory domain are electrically connected. The composite of the screw and the microphone as a single multimodal tactile sensing module simplifies a practical fabrication process and makes the system robust since no electronic or transducer is exposed to external impact. Such a module is installed on multiple points on the sensory domain to measure a conductivity change between pairs of electrodes and a micro-vibration at an arbitrary location.

C. Fabrication process

The outer multilayered fabric and the conductive sensory domain with multimodal sensing modules are fabricated simultaneously and combined to comprise the developed robotic skin. The overall sensor structure is shown in Fig. 2.

The conductive sensory domain is made of an acrylic plate, which is rigid enough to maintain the structure and tolerate impulsive stimuli. Twenty-five counterbore holes are made on the acrylic plate to keep the sensing domain flat when vented screws are fastened on the plate with nuts. An ABS housing is made with a 3D printer (F170, Stratasys, USA) to attach a microphone (CMEJ-4622-25-L082, CUI Devices, USA) to each screw. The microphone is attached to the housing with an epoxy adhesive (Sil-Poxy, Smooth-on, USA), and the housing is fixed to a nut with an instant adhesive (Loctite 401, Loctite, Germany), completing a single multimodal tactile sensing module. Such a sensing module is installed in the counterbore holes, resulting in a 5×5 square lattice with a spacing of 50 mm. A carbon nanotube (CNT) solution (Graphit 33, Kontakt Chemie, Germany) is sprayed several times on the plate until a conductive network is achieved. A silver paste (ELCOAT P-100, CANS, Japan) is applied between the vented screws and the plate to establish a stable electrical connection between the CNT-coated conductive sensory domain and the electrodes.

The outer multilayered fabric is a composite of loop fabric-attached neoprene (CN3, Soitex, Korea), a non-conductive fabric, and a highly conductive fabric (BTL-1, Soitex, Korea). The conductive fabric is cut by a laser cutter (Speedy 300, Trotec, USA) into an array of grid patches and adhered to a non-conductive fabric layer to preserve the patches' location and shape. An additional layer of non-conductive fabric is cut in the counter-shape of the patches and placed along with the patches, making the contact surface flat. The

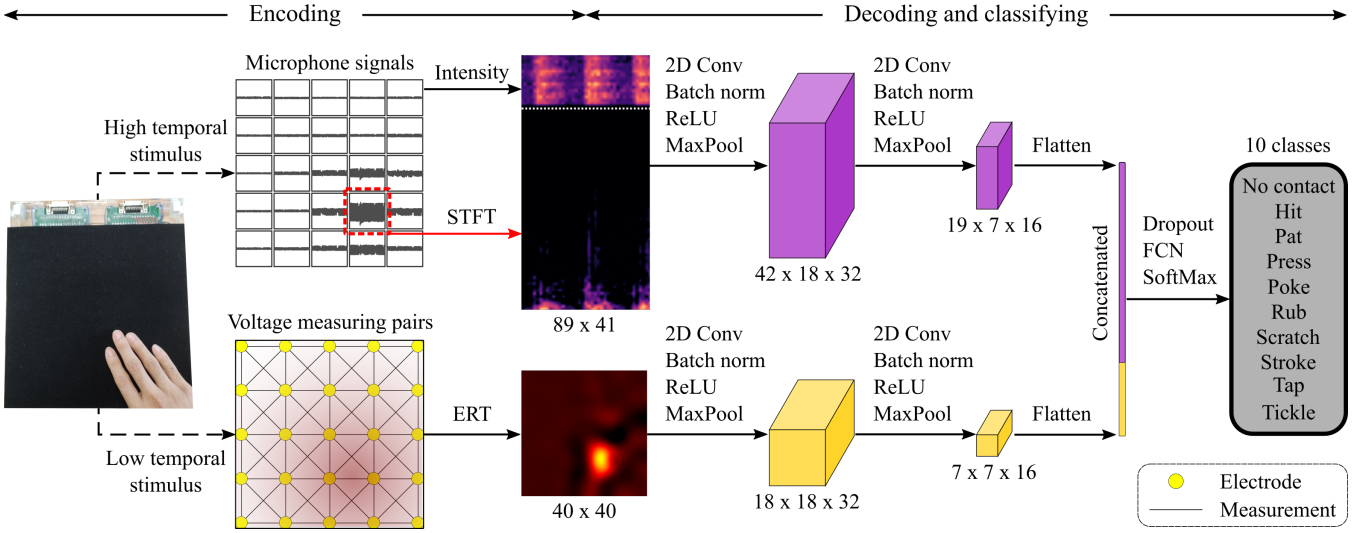

Fig. 4: Feature maps construction to encode spatiotemporal information of touch, and the CNN structure to classify the touch into ten classes.

conductive fabric patches and the non-conductive fabrics were attached using a polyurethane (PU) film (Stars HTV Seoul, South Korea). The PU film is a light and flexible adhesive, activated by the heat of about 200 °C. It is heated with an iron to attach the fabrics while maintaining their elasticity. The neoprene with loop fabric is then attached to the non-conductive fabric layer with the instant adhesive to comprise the multilayered fabric. The resulting fabric is about 4 mm thick and is fixed to the conductive sensory domain of the acrylic plate by applying the instant adhesive only to the border of the multilayered fabric in order to give sufficient adhesion without interrupting the piezoresistive structures of the sensor.

The electrodes and microphones are connected to a single data acquisition (DAQ) device (myRIO-1900, National Instruments, USA) via custom multiplexing boards. The electrodes are connected to pairs of analog outputs and inputs, each injecting a current between an arbitrary electrode pair and measuring the corresponding voltage. Instead of a constant current source, a constant voltage source is used as the input with a serially connected reference resistor to measure a voltage between the electrodes indirectly. The microphones are connected to high pass filters and analog inputs to remove any offset and measure microphone signals. A field-programmable gate array (FPGA) of the DAQ controls the multiplexing boards to sample at high speed, achieving 15 μs for a single current injection and voltage measurement and 10 kHz of sampling rate per microphone.

III. Touch Sensibility Validation

A force of typical touches in human physical interaction ranges between 0.3 N and 10 N [5], and mechanoreceptors in human skin can sense a high temporal stimulus up to 1000 Hz [22]. A cyclic loading and a vibratory stimulus in such ranges are applied to the developed skin to validate its sensibility to social touches.

A. High temporal sensibility

A sensibility to a high temporal component of touch is validated by applying a vibratory stimulus using a shaker (Mini-shaker type 4810, Bruel & Kjaer, Denmark). A tip of the shaker is placed on the skin directly above a sensing module, and a chirp signal ranging from 1 Hz to 1 kHz is applied in a linear slope using a function generator (AFG 3022, Tektronix, USA). The chirp signal sweep time is 10 s, and a peak-to-peak voltage is 10 V. The microphone signal is logged during stimulation and repeated once again while the shaker tip is in the air to record an acoustic noise measured by the microphone under the identical stimulus. With the known profile of the chirp signal, a signal-to-noise ratio (SNR) is computed about stimulus frequency, as shown in Fig. 3a. The sensing module can sense an upper limit of human sensibility to high temporal stimuli and has a limit of detection of about 38 Hz, a point where a signal is three times the noise's standard deviation.

B. Low temporal sensibility

A sensibility to a low temporal component of touch is validated by applying a cyclic load. A mechanical impedance sensor (Model 288D01, PCB Piezotronics, USA) is placed on the midpoint of neighbouring sensing modules and cyclically indented the skin using a motorised indentation setup (EzROBO-5GX ST3030, Iwashita Engineering, Japan). The indentation depth is about 4 mm, equivalent to the outer fabric's thickness, with a speed of 3.5 mm/s, and kept the pressure for 0.5 s before unloading with the same speed. A current is injected into the electrode pair during the indentation, and the corresponding voltage change is normalised about a voltage across the reference resistor. The force applied to the skin and low pass filtered normalised voltage change are measured, as shown in Fig. 3b. The developed skin is robust to a low temporal force of about 12 N. A conductivity between the modules changes as the

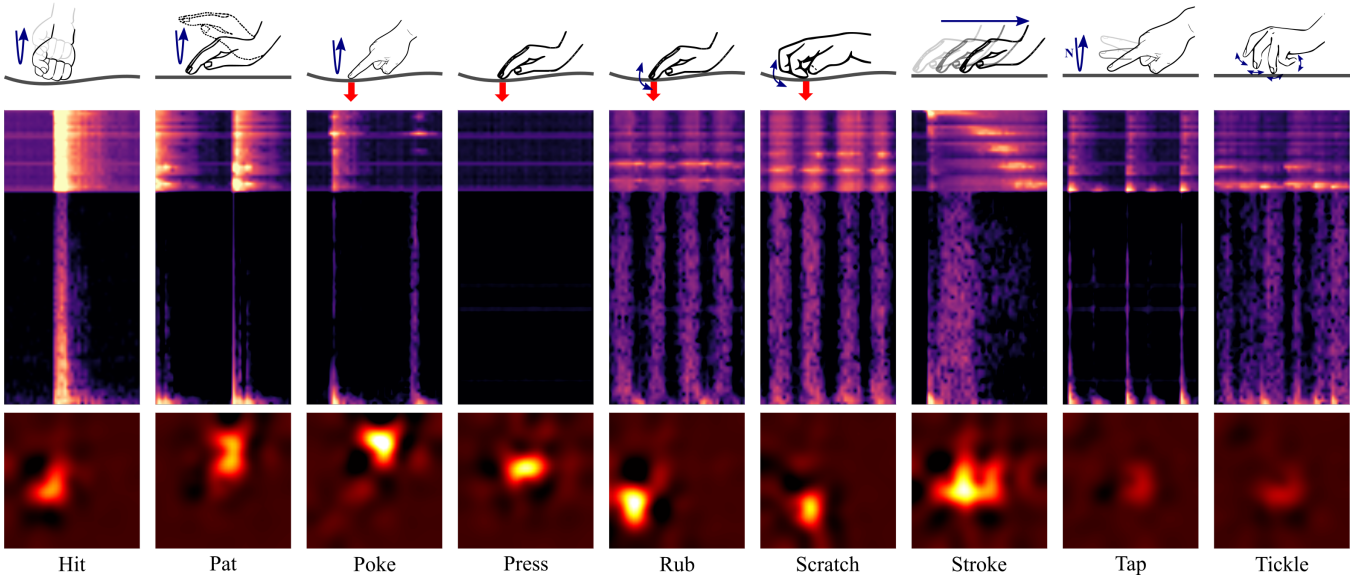

Fig. 5: Example feature maps of nine touch modalities. The upper row is constructed from high temporal components measured with microphones, and the lower row is constructed from low temporal components measured with electrodes.

force deforms the skin but saturates after about 1 s, which corresponds to 3.5 mm indentation, and the applied force is about 9.7 N.

IV. Touch Modality Classification

Microphones and electrodes can sense high and low temporal components of touch, respectively, where each is independently processed to encode temporal and spatial information into a feature map. A convolutional neural network (CNN) is trained to classify feature maps of baseline noise and nine touch modalities selected from a touch dictionary [8], as shown in Table. I.

A. Feature maps construction

A feature map of a high temporal touch component is composed of two sub-maps and computed from the latest 512 ms microphones signals, which is equivalent to 5120 samples per microphone. The first sub-map is time-windowed intensities of microphones' signals. A microphone's intensity depends on the distance between the sensing module and a touch point; thus, the sub-map encodes amplitude and time-varying spatial information of the touch's high temporal component. The second sub-map is a spectrogram of the microphone signal with the largest intensity to encode a temporal property over time. Only the largest signal is employed since it would be closest to the touch, thus least attenuated during propagation. A short-time Fourier transform (STFT) for spectrogram computation has a time window length and stride length of 128 samples, which is also employed in time-windowed intensities computation in the first sub-map. Therefore the sub-maps have an equal length along a time axis, thus concatenated to form a final feature map of 89×41.

A feature map of a low temporal touch component is a reconstructed image of conductivity change of the skin's conductive domain. An electrical resistance tomography (ERT) is employed to estimate the conductivity change from voltage measurements between electrode pairs. An open-source library (EIDORS) is used to define the Jacobian-based linearised model of a voltage change about a conductivity perturbation. Its inverse problem is a linearised reconstruction matrix of the conductivity change from the voltage change, but it is ill-posed; thus, a Laplacian-type regularisation prior is used [23]. Therefore, matrix multiplication of the reconstruction matrix and the measured voltage change computes an estimation of the conductivity change map, which encodes an amplitude and spatial information of a low temporal component of touch. A current injection and resulting voltage change are measured only from 72 selected electrode pairs, as shown in Fig 4, based on an optimisation method [24]. The corresponding reconstruction matrix is computed and multiplied with the measured voltage changes, resulting in a 40×40 feature map. Two feature maps are simultaneously computed at a rate of 10 Hz, and example feature maps of nine touch modalities are shown in Fig. 5.

B. Classification using CNN

Spatiotemporal information encoded as the feature maps is decoded and classified using a 2D CNN, as shown in Fig. 4. Each feature map undergoes identical layers with two convolutional layers. Kernels of the convolutional layers are $5\times5\times32$ and $5\times5\times16$, in computation order, with a stride of one and no padding. Each convolutional layer is followed by a batch normalisation layer, a rectified linear unit activation layer, and a max-pooling layer with a size and stride of two. The outputs are flattened and concatenated and go through a dropout layer with a probability of 0.2, followed by a fully connected layer and a SoftMax layer to classify a touch into ten classes; nine classes for each touch modality and an additional class for the rest state where no contact is made.

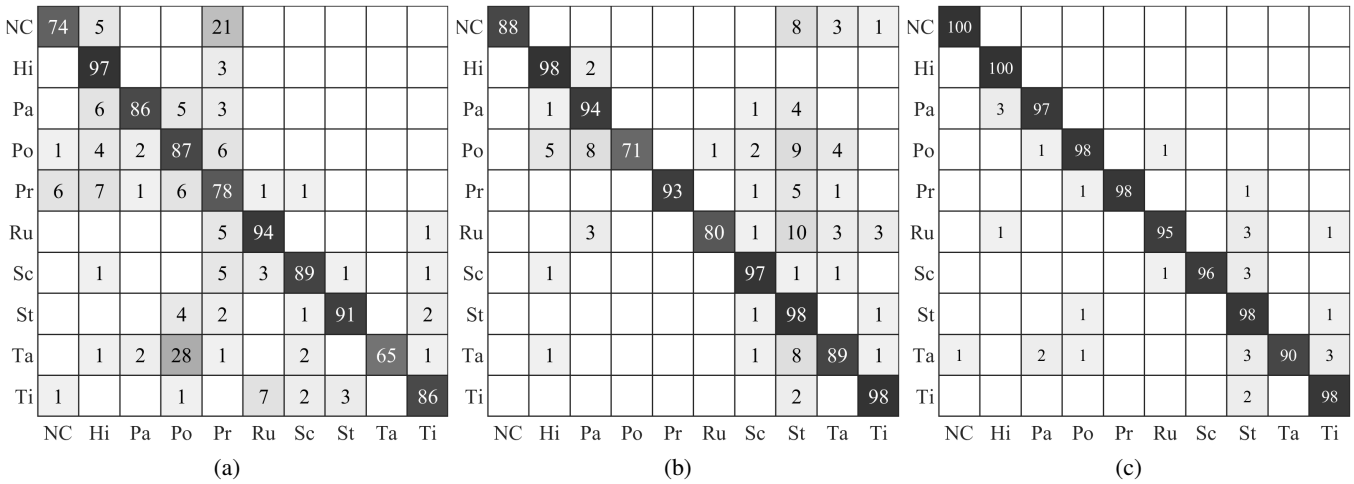

Fig. 6: Confusion matrices on classifying the test set when the network is (a) trained only with high temporal feature maps, (b) trained only with low temporal feature maps, and (c) trained with both features maps. Networks achieved an accuracy of 84.7 %, 90.6 %, and 97.0 %, respectively. Ten classes in abbreviations: NC, no contact; Hi, hit; Pa, pat; Po, poke; Pr, press; Ru, rub; Sc, scratch; St, stroke; Ta, tap; Ti, tickle.

A dataset of feature maps is collected to train and test the network. Three individuals are presented with Table I and asked to apply nine touch modalities to the developed skin until 1000 feature map pairs are recorded for each touch. 1000 feature map pairs of baseline noise are also collected for the rest state. The collected dataset is randomly divided into training, validation, and test sets at a ratio of 8:1:1, and the train set is augmented by a factor of 20 by adding Gaussian noise, resulting in 16,000 training samples. The network is trained using an adaptive moment estimation (ADAM) optimiser with an initial learning rate of 0.0002, which drops with a factor of 0.1 every five epochs. A mini-batch size is 64, and a validation loss is computed every 50 iterations. The training aborts if the validation loss does not decrease for 20 consecutive times or reach a maximum epoch of 20. The network is trained with a single GPU (GeForce RTX 3070 8GB, NVIDIA, USA).

Three networks with identical structures are trained, where two are each trained with the high temporal feature maps or the low temporal feature maps solely, and the third is trained using both feature maps. The three networks classified the test set, and each achieved an accuracy of 84.7 %, 90.6 %, and 97.0 %, respectively, as shown in Fig. 6. The network trained only with the high temporal feature maps confuses a press and rest state since the press is a low temporal touch; therefore, no signal is measured by the microphones and is hardly distinguished from the baseline. Similarly, the network trained only with the low temporal feature maps confuses a stroke and poke, whereas the network trained with both feature maps outperformed the two networks.

V. Conclusion and Discussion

This paper presented a robotic skin with multimodal tactile sensing modules to sense and classify various touch modalities. The skin can sense high temporal vibration between 38 Hz and 1 kHz, which covers an upper limit of a human skin sensibility. Also, the skin is robust to a low temporal cyclic force up to 12 N. However, the skin could hardly measure a vibration beneath 20 Hz, and the conductivity change is saturated about a force beyond 9.7 N. The lower vibration sensitivity bound is caused by a condenser microphone's frequency bandwidth limitation. The saturation of conductivity change in cyclic loading is due to the multilayered fabric structure. Once a conductive patch is compactly pressed against the conductive domain, no additional deformation and conductivity change can occur beyond the point. Such saturation may be improved by changing the mechanical property of the multilayered fabric by employing a fabric with a higher elastic modulus.

Even though the skin has some limitations in sensibility, it could sense wide temporal components of touch and encode its spatiotemporal information into two feature maps. This paper demonstrated that both high and low temporal sensibilities are required to well classify various touches. The skin achieved a high accuracy of 97.0 % but has room for improvement since some touch modalities, such as pinch, are implausible due to the limited skin stretchability and vulnerable to a loud acoustic noise due to the use of a microphone. Yet, the developed skin is applicable for an intuitive pHRI with its various beneficial characteristics that could not be simultaneously achieved in previous works; a few simple and unified multimodal sensing modules makes the fabrication process simple and reduces power consumption; flexible and light multilayered fabric covering the sensing modules makes the skin easily conformable to a larger scale and robust to external impact and extreme touch modality such as hit; and a touch classification in real-time.

Acknowledgment

This work was supported by a National Research Foundation of Korea (NRF) grant funded by the Korean government (MEST) (No. NRF-2021R1A2C2093660)

REFERENCES

[1] J. B. Van Erp and A. Toet, "Social touch in human–computer interaction," *Frontiers in digital humanities*, vol. 2, p. 2, 2015.

[2] A. Debrot, D. Schoebi, M. Perrez, and A. B. Horn, "Touch as an interpersonal emotion regulation process in couples' daily lives: The mediating role of psychological intimacy," *Personality and Social Psychology Bulletin*, vol. 39, no. 10, pp. 1373–1385, 2013.

[3] A. Dagnino-Subiabre, "Resilience to stress and social touch," *Current Opinion in Behavioral Sciences*, vol. 43, pp. 75–79, 2022.

[4] M. J. Hertenstein, R. Holmes, M. McCullough, and D. Keltner, "The communication of emotion via touch." *Emotion*, vol. 9, no. 4, p. 566, 2009.

[5] D. Silvera-Tawil, D. Rye, and M. Velonaki, "Artificial skin and tactile sensing for socially interactive robots: A review," *Robotics and Autonomous Systems*, vol. 63, pp. 230–243, 2015.

[6] P. Delmas, J. Hao, and L. Rodat-Despoix, "Molecular mechanisms of mechanotransduction in mammalian sensory neurons," *Nature Reviews Neuroscience*, vol. 12, no. 3, pp. 139–153, 2011.

[7] R. Dahiya, N. Yogeswaran, F. Liu, L. Manjakkal, E. Burdet, V. Hayward, and H. Jörntell, "Large-area soft e-skin: The challenges beyond sensor designs," *Proceedings of the IEEE*, vol. 107, no. 10, pp. 2016–2033, 2019.

[8] S. Yohanan and K. E. MacLean, "The role of affective touch in human-robot interaction: Human intent and expectations in touching the haptic creature," *International Journal of Social Robotics*, vol. 4, no. 2, pp. 163–180, 2012.

[9] R. Andreasson, B. Alenljung, E. Billing, and R. Lowe, "Affective touch in human–robot interaction: conveying emotion to the nao robot," *International Journal of Social Robotics*, vol. 10, no. 4, pp. 473–491, 2018.

[10] Y. Zhou, T. Kornher, J. Mohnke, and M. H. Fischer, "Tactile interaction with a humanoid robot: Effects on physiology and subjective impressions," *International Journal of Social Robotics*, vol. 13, no. 7, pp. 1657–1677, 2021.

[11] Y. S. Sefidgar, K. E. MacLean, S. Yohanan, H. M. Van der Loos, E. A. Croft, and E. J. Garland, "Design and evaluation of a touch-centered calming interaction with a social robot," *IEEE Transactions on Affective Computing*, vol. 7, no. 2, pp. 108–121, 2015.

[12] N. Geva, F. Uzefovsky, and S. Levy-Tzedek, "Touching the social robot paro reduces pain perception and salivary oxytocin levels," *Scientific reports*, vol. 10, no. 1, pp. 1–15, 2020.

[13] C. Bartolozzi, L. Natale, F. Nori, and G. Metta, "Robots with a sense of touch," *Nature materials*, vol. 15, no. 9, p. 921, 2016.

[14] A. Dabbous, A. Ibrahim, M. Valle, and C. Bartolozzi, "Touch modality classification using spiking neural networks and supervised-stdp learning," in *2021 28th IEEE International Conference on Electronics, Circuits, and Systems (ICECS)*. IEEE, 2021, pp. 1–4.

[15] D. Silvera Tawil, D. Rye, and M. Velonaki, "Interpretation of the modality of touch on an artificial arm covered with an eit-based sensitive skin," *The International Journal of Robotics Research*, vol. 31, no. 13, pp. 1627–1641, 2012.

[16] P. Gastaldo, L. Pinna, L. Seminara, M. Valle, and R. Zunino, "A tensor-based approach to touch modality classification by using machine learning," *Robotics and Autonomous Systems*, vol. 63, pp. 268–278, 2015.

[17] M. J. Yang, K. Park, and J. Kim, "A large area robotic skin with sparsely embedded microphones for human-robot tactile communication," in *2021 IEEE International Conference on Robotics and Automation (ICRA)*. IEEE, 2021, pp. 3248–3254.

[18] D. Silvera-Tawil, D. Rye, M. e. Soleimani, and M. Velonaki, "Electrical impedance tomography for artificial sensitive robotic skin: A review," *IEEE Sensors Journal*, vol. 15, no. 4, pp. 2001–2016, 2014.

[19] Z. Kappassov, J.-A. Corrales, and V. Perdereau, "Tactile sensing in dexterous robot hands," *Robotics and Autonomous Systems*, vol. 74, pp. 195–220, 2015.

[20] M. Kaboli, A. Long, and G. Cheng, "Humanoids learn touch modalities identification via multi-modal robotic skin and robust tactile descriptors," *Advanced Robotics*, vol. 29, no. 21, pp. 1411–1425, 2015.

[21] K. Park, H. Park, H. Lee, S. Park, and J. Kim, "An ert-based robotic skin with sparsely distributed electrodes: Structure, fabrication, and dnn-based signal processing," in *2020 IEEE International Conference on Robotics and Automation (ICRA)*. IEEE, 2020, pp. 1617–1624.

[22] S. Bolanowski Jr and J. J. Zwislocki, "Intensity and frequency characteristics of pacinian corpuscles. i. action potentials," *Journal of neurophysiology*, vol. 51, no. 4, pp. 793–811, 1984.

[23] D. S. Tawil, D. Rye, and M. Velonaki, "Improved image reconstruction for an eit-based sensitive skin with multiple internal electrodes," *IEEE Transactions on Robotics*, vol. 27, no. 3, pp. 425–435, 2011.

[24] K. Park, H. Lee, K. J. Kuchenbecker, and J. Kim, "Adaptive optimal measurement algorithm for ert-based large-area tactile sensors," *IEEE/ASME Transactions on Mechatronics*, vol. 27, no. 1, pp. 304–314, 2021.